Defence Science Journal, Vol. 69, No. 3, May 2019, pp. 303-310, DOI : 10.14429/dsj.69.13636

Selection of Pressure Angle-based on Dynamic Effects in Asymmetric Spur Gear with Fixed Normal Contact Ratio

Benny Thomas[#,*], K. Sankaranarayanasamy[@], S. Ramachandra[#], and S.P. Suresh Kumar[#]

[#]*DRDO-Gas Turbine Research Establishment, Bengaluru - 560 093, India*
[@]*National Institute of Technology, Tiruchirapalli - 620 015, India*
[*]*E-mail: bennythomas@gtre.drdo.in*

ABSTRACT

Asymmetric spur gears are finding application in many fields including aerospace propulsion and automobile which demand unidirectional or relatively higher load on one side of the gear flank. Design intend to maximise the load carrying capacity of the drive side of asymmetric gear by increasing the pressure angle is achieved at the expense of coast side capacity. Multiple solution for coast to drive side pressure angle exist for a given contact ratio and each of these have relative merits and demerits. In the present work asymmetric spur gears of theoretically equal contact ratio as that of corresponding symmetric gears are selected to investigate the change in gear tooth static transmission error and dynamic behaviour with coast and drive side pressure angle. Study shows that dynamic factor of normal contact ratio asymmetric spur gears below resonance speed are relatively lower than corresponding symmetric gears of same module, contact ratio, number of teeth, coast side pressure angle and fillet radii. Results also show that, coast and drive side pressure angle can be suitably selected for a given contact ratio to reduce the single tooth and double tooth contact static transmission error and dynamic factor of asymmetric spur gears.

Keywords: Asymmetric gear; Non-extended contact; Extended contact; Contact ratio; Mesh stiffness; Static transmission error; Dynamic factor

NOMENCLATURE

b_{fw}	Gear tooth face width (mm)
b_h	Full Hertzian contact width (m)
c	Length of the element normal to the loaded edge (m)
c_m	Damping coefficient in N-m/s
e	Element dimension along the loaded edge (m)
hf_{ac}	Tool addendum coefficient
hf_{dc}	Tool dedendum coefficient
E	Young's modulus (N/m^2)
F_D	Dynamic load (N)
F_{nL}	Normal gear tooth load per unit face width (N/m)
F_{ST}	Static gear tooth load (N)
J	Mass moment of inertia (kgm^2)
k_j	Single gear tooth stiffness corresponding to the jth point of load application (N/m)
k_{tot}	Total mesh stiffness (N/m)
m	Module
m_a	Top land thickness factor
M	Mass of the gear (kg)
R	Pitch circle radius (mm)
R_b	Base circle radius of drive side (m)
R_r	Relative radius of curvature at the contact point (mm)
T	Torque (Nm)
TR	Tool tip radius
$V_{e/s}$	Entraining to sliding velocity
v_s	Sliding velocity (mm/s)
y	Linear displacement (m)
z	Number of gear tooth
x_d	Relative displacement along the line of action (m)
$\dot{x}_d$	Relative velocity along the line of action (m/s)
$\ddot{x}_d$	Relative acceleration along the line of action (m/s^2)
x_s	Static transmission error (m)
z, z_t	Number of gear tooth
α	Pressure angle (degree)
δ_j	Gear tooth deflection along the line of action at jth point on tooth profile due to F_n (m)
θ	Angular displacement (rad)
$\ddot{\theta}$	Angular acceleration (rad/s^2)
ρ	Roll distance (m)
ν	Kinematic viscosity in centistokes
ϑ	Poisson's ratio
ζ	Damping ratio
ω	Frequency during the meshing period (Hz)
μ	Coefficient of friction

Subscript

c	Coast side
d	Drive side
I, II	Mesh pair I,II
p, g	Pinion , Gear

Received : 26 September 2018, Revised : 14 January 2019
Accepted : 22 January 2019, Online published : 30 April 2019

1. INTRODUCTION

The need to enhance the life and performance of mechanical power transmission devices has lead to development of new and unconventional designs, such as asymmetric gears. As the name implies the drive and coast side profiles in these gears are not symmetric. This type of gear can be beneficially put to application where the load on one side is relatively higher than the other side. Gears with asymmetric teeth were successfully put to use in the planetary gearbox of TV7-117S turboprop engine. Researchers have demonstrated enhanced performance of helicopter main drive gears designed with asymmetric profile. These gears were required to transmit higher load for a longer duration on one flank relative to the other. Asymmetric gear tooth designed with suitable flexibility has found application in gear pumps due to higher output pressure, flow, and efficiency compared to conventional gear pumps. Need to maximise the power density, operational speed, life and performance of transmission systems have drawn the interest of many researchers to study the dynamics of asymmetric spur gear tooth. Studies have suggested the use of asymmetric spur gears with contact ratio close to two or high contact ratio (HCR) gears to minimise the dynamic factor. It is known that HCR spur gears have relatively high power loss compared to normal contact ratio (NCR) gears and many applications do not demand use of HCR asymmetric spur gears. In such cases, designers have the challenging task of selecting coast and drive side pressure angle for a given contact ratio meeting the stress, noise and vibration criterion all of which are influenced by the dynamic behaviour of gear tooth.

Kapelevich and Roderick[1] presented the procedure for designing asymmetric spur gears using generating rack profile. Thomas[2], *et al.* introduced novel search method to analytically compute the gear tooth bending stress in normal contact ratio asymmetric spur gears. Hsi[3], *et al.* analytically determined the tooth stiffness and computed the dynamic behaviour of gear system. They found that the dynamic factor (DF) reduced with increase in load. Rincon[4], *et al* decomposed gear tooth deformation into local and global deformations to determine the mesh stiffness. Authors claimed this approach to be much faster than conventional FE models with contact elements. Niels[5], *et al.* determined the gear tooth stiffness as a function of contact position and found that the stiffness is nearly linear when expressed in the involute arc length of teeth. Karpat[6,7], *et al.* developed equations based on extensive FE analysis to determine the tooth stiffness of symmetric and asymmetric spur gears with defined gear tooth parameters.

Tamminana[8], *et al.* predicted the dynamic behaviour of symmetric spur gear pairs using a developed deformable-body model and a simplified discrete model. Finding of the analytical study was experimentally validated. Vedmar[9], *et al.* considered the elasticity coupling and off line-of-action (OLOA) in gear dynamics study. Their study showed that the dynamic factors were relatively low compared to line of action (LOA) approach. Change in static transmission error (STE) due to gear tooth deflections in symmetric spur gear was predicted by Lin[10], *et al.* Effect of the extended tooth contact (ETC) was studied to assess the influence on the dynamic factor and critical speed. Their studies showed that neglecting the ETC effect results in underestimating resonant speeds and overestimating dynamic loads. John[11], *et al.* performed detailed studies to arrive at the optimal element size to determine the gear tooth deflections at the point of load application. Kasuba[12], *et al.* modelled the gear train as a rotating system excited with variable-variable mesh stiffness. Variability in mesh stiffness due to the transmitted load, gear tooth deflections, gear hub torsional deflections and position of contacting profile points were determined. It was demonstrated in the study that certain profile error and pitting can induce interruptions of gear mesh stiffness that could increase the dynamic load. Lin[13], *et al* performed the gear dynamic analysis by considering the effects due to flexibility of shafts and bearings. Parametric studies on gears showed that dynamic factor reached considerably low value at contact ratio of two and damping has a major influence on dynamic factor close to critical speed. Osire[14,15,16], *et al.* performed studies on the dynamic behaviour of asymmetric and symmetric spur gears under non-extended tooth contact (NETC) condition and showed that asymmetric spur gears have higher dynamic factor when compared to symmetric spur gears with same gear parameters. This difference in dynamic factor is due to the lower contact ratio of asymmetric spur gears when compared to symmetric spur gears of same gear tooth parameters.

Survey shows that systematic comparative studies on dynamic factor of asymmetric and symmetric spur gears of same contact ratio have not been attempted. Intention of the present study is to compare the dynamic behaviour of NCR, symmetric and asymmetric spur gears of given contact ratio. Results of this study are used to analytically identify the preferred choice of drive and coast side pressure angle in the selected gears to reduce the static transmission error and dynamic factor. Computational investigation is also made in this work to assess the influence of extended tooth contact (ETC) on time varying mesh stiffness (TVMS) and DF.

2. DETERMINATION OF SINGLE GEAR TOOTH STIFFNESS

Determination of single gear tooth stiffness is the first step to compute the mesh stiffness, dynamic load and dynamic factor. Single tooth stiffness corresponding to any point on the gear tooth profile is calculated from the total deflection along the line of action due to the application of a specified normal tooth load (F_n) at that point.

2.1 FE Method for Single Gear Tooth Stiffness Prediction

In the present work, spur gear pairs with zero backlash, same contact ratio and tooth parameters as given in Table 1 are selected to study the dynamic behaviour. Figure 1 shows the basic rack profile of asymmetric gear.

Matlab codes were developed to generate the involute and fillet profile of asymmetric gear which was further used to develop the finite element model in Hyperworks. 2D meshed models are used in this study to determine the gear tooth deflection at the point of load application.

Assumptions[2] made in the FEA are as follows:

1. Material is linear, elastic, isotropic and homogeneous with Poisson's ratio= 0.3

Table 1. Gear tooth pairs used to study dynamic effects

Gear pair identification number	1	2	3	4	5	6	7
Number of tooth	32	40	40	40	40	40	40
Gear ratio	1	1	1	1	1	1	1
Module m (mm)	3.18	2	2	2	2	2	2
Tool addendum coefficient hf_{ac}	1.25	1.176	1.44	1.44	1.44	1.46	1.48
Face width b_{fw} (mm)	25.4	25	25	25	25	25	25
Tool tip radius $TR_{d,c}$ (mm)	0.3	0.1	0.1	0.1	0.1	0.1	0.1
Coast side pressure angle α_c (degree)	20°	20°	20°	17°	13°	17°	13°
Drive side pressure angle α_d (degree)	20°	20°	31°	31°	31°	32.3°	33.9°
Young's Modulus (GPa)	215	210	210	210	210	210	210
Mass (kg)	0.7	1	1	1	1	1	1
Contact ratio	1.667	1.6	1.6	1.6	1.6	1.6	1.6
Applied normal tooth load (N)	1250	2660	2916	2916	2916	2959	3012

2. Uniform load distribution along the face width of the gear tooth
3. Gear tooth is free of errors

Equation (1), as suggested by authors[11], gives the relation between the element size and aspect ratio to be maintained in the FE model when the gear tooth contact is represented using a concentrated load to determine the deflection within the interval of definition

$$\frac{e}{b_h} = -0.2\left(\frac{c}{e}\right) + 1.2, \quad 0.9 < \frac{c}{e} < 3 \tag{1}$$

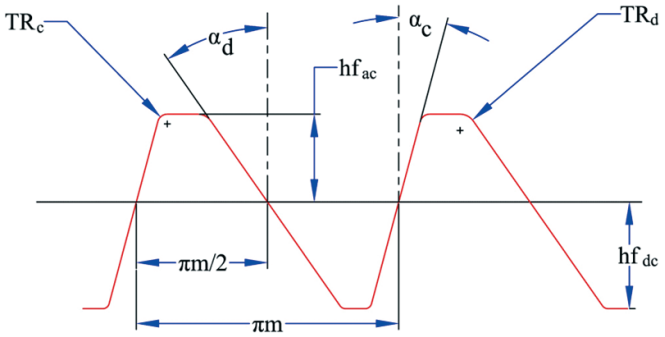

Figure 1. Basic rack profile for asymmetric gear.

Gear tooth parameters and finite element edge length used in the present study are shown in Figs. 2(a) and 2(b). Figure 2(c) shows the FE model of 17°/31° coast to drive side pressure angle asymmetric spur gear used to compute gear tooth deflection when a concentrated load is applied at highest point of single tooth contact.

Single tooth stiffness (N/m) for the pinion (k_{jp}) and gear (k_{jg}) corresponding to the j[th] point of load application is given by :

$$k_{jp,jg} = \frac{F_n}{\delta_{jp,jg}} \tag{2}$$

3. TIME VARYING MESH STIFFNESS UNDER NETC CONDITION

TVMS is computed using the single tooth stiffness predicted through FE analysis in the previous section. Mesh stiffness of the i[th] mesh pair at the j[th] point of contact (k_{ji}) is given as

$$k_{ji} = \frac{k_{jgi}k_{jpi}}{k_{jgi} + k_{jgi}} \tag{3}$$

Total mesh stiffness (k_{tot}) of normal contact ratio (NCR) asymmetric spur gear at the j[th] pair of contact point for DTC (double tooth contact) or j[th] contact point for STC (single tooth contact) is given by

$$k_{tot} = \begin{bmatrix} \sum_{i=I,II} k_{ji} \; for \; DTC \\ \sum_{i=I} k_{ji} \; for \; STC \end{bmatrix} \tag{4}$$

4. EXTENDED CONTACT

For extended tooth contact condition, the mesh stiffness and STE under NETC condition is suitably modified to introduce the effect due to early start of contact and delayed end of contact. STE at the extended contact region on the recess side $(STEr)_j$ and approach side $(STEa)_j$ for the j^{th} pair of contact for double tooth contact is given by

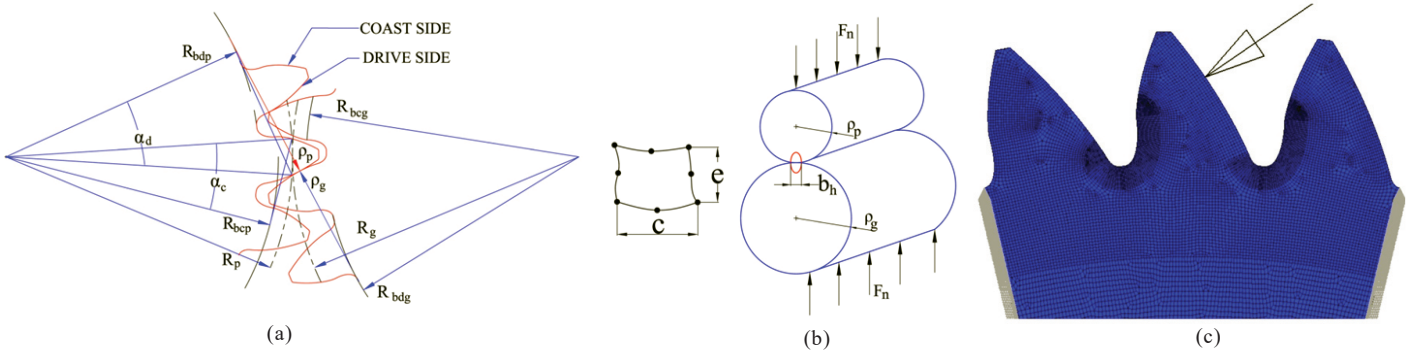

Figure 2. Gear parameters, element edge length and FE model (a) Gear parameters for tooth stiffness calculation, (b) Higher order 2D quad-element with edge length and hertzian contact zone due to normal tooth load F_n, and (c) Finite element model of 17°/31° coast to drive side pressure angle asymmetric spur gear.

$$(STEr)_j = \frac{\left(\frac{(SPr^{aa})_j}{(k^{bb})_j} + \frac{F_n}{(k^{aa})_j (k^{bb})_j}\right)}{\left(\frac{(k^{aa})_j + (k^{bb})_j}{(k^{aa})_j (k^{bb})_j}\right)} \quad (5)$$

$$(STEa)_j = \frac{\left(\frac{(SPr^{cc})_j}{(k^{bb})_j} + \frac{F_n}{(k^{cc})_j (k^{bb})_j}\right)}{\left(\frac{(k^{cc})_j + (k^{bb})_j}{(k^{cc})_j (k^{bb})_j}\right)} \quad (6)$$

where *aa* corresponds to the recess pair, *bb* denotes the gear pair under study and *cc* denotes the approaching pair. $(STEr)_j$ is the STE due to j^{th} point of contact on gear pair *bb* and corresponding recess pair *aa*. $(STEa)_j$ is the STE due to j^{th} point of contact on gear pair *bb* and corresponding approach pair *cc*. $(SPr^{aa})_j$ and $(SPr^{cc})_j$ are the theoretical separation between the tooth pair aa and *cc* at the recess and approach side respectively corresponding to j^{th} pair of contact.

5. GEAR DYNAMICS

In this study lumped parameter dynamic model shown in Fig. 3 is used to analyse spur gear tooth dynamics. Gear wheels in mesh represented by rigid wheels are connected by (i) spring elements with time varying mesh stiffness (k_I and k_{II} in N/m); and (ii) damper of damping coefficient c_m (N-m/sec) to represent energy losses at the gear mesh. Y axis of the rectangular coordinate system in this model is chosen along the line of action.

Formulation for equations of motion may be written as:

$$J_g \ddot{\theta}_g = R_{bdg}(F_{DI} + F_{DII}) - R_{bdg} F_{ST} \pm \rho_{gI} \mu_I F_{DI} \pm \rho_{gII} \mu_{II} F_{DII} \quad (7)$$

$$J_p \ddot{\theta}_p = -R_{bdp}(F_{DI} + F_{DII}) + R_{bdp} F_{ST} \pm \rho_{pI} \mu_I F_{DI} \pm \rho_{pII} \mu_{II} F_{DII} \quad (8)$$

$$F_{ST} = \frac{T_g}{R_{bdg}} = \frac{T_p}{R_{bdp}} \quad (9)$$

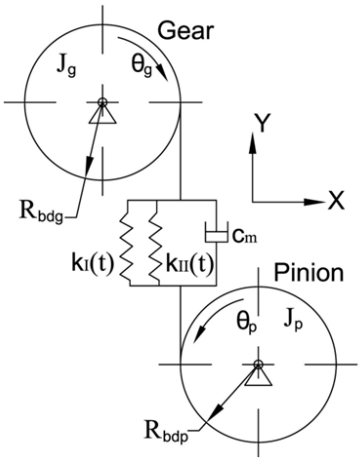

Figure 3. Lumped parameter dynamic model of asymmetric spur gear tooth.

In the rectangular coordinate system, the linear displacement $y_{p,g}$ and relative displacement along the line of action due to angular displacement $\theta_{p,g}$ can be expressed as

$$y_{p,g} = R_{bdp,g} \theta_{p,g} \quad (10)$$

$$x_d = R_{bdp} \theta_p - R_{bdg} \theta_g \quad (11)$$

Coefficient of friction derived by Dowson and Higginson used in this study is given by

$$\mu = 18.175 \nu^{-0.15} |V_{e/s}|^{-0.15} |v_s|^{-0.5} (R_r)^{-0.5} \quad (12)$$

Mass moment of inertia of the gear and pinion wheels can be expressed as

$$J_g = M_g (R_{bdg})^2 \quad (13)$$

$$J_p = M_p (R_{bdp})^2 \quad (14)$$

Equation (15) gives the reduced form of Eqns. (7) and (8) in the rectangular coordinate system by substituting the expression for mass moment of inertia in Eqns. (13) and (14) and coefficient of friction μ from Eqn. (12).

$$\ddot{x}_d + 2\omega\zeta\dot{x}_d + \omega^2 x_d = \omega^2 x_s \quad (15)$$

Equation (15) is numerically solved using fourth order Runge-Kutta method. In the numerical solution damping ratio (ζ) of 0.17 and kinematic viscosity (ν) of 100cSt is assumed and the mesh period is divided into 500 points to improve the accuracy of transition points. Solution for the equation is obtained iteratively for an assumed initial value of x_d and $\dot{x}_d$. Iteration is repeated till the ratio of the difference between the initial value and the value at the end of single tooth contact to the initial value drops below 0.00001.

Total dynamic load acting on the gear under the assumption that the gear tooth profile is free of errors is given by

$$F_{Dtot} = k_{tot} x_d + c_m \dot{x}_d \quad (16)$$

Total dynamic gear tooth mesh load can be calculated from Eqn. (16) to a good degree of accuracy by neglecting the damping force as this term is relatively small in magnitude compared to mesh stiffness force.

To verify the analytical procedures presented in this section, dynamic study is performed on the first gear tooth pair in Table 1. Figure 4(a) is the static and dynamic load acting on the gear tooth at 2000 rpm and Fig. 4(b) presents the dynamic factor from 100 rpm to 20000 rpm for gear pair 1 (mass 1.2 kg). Results on the dynamic load and dynamic factor show good agreement with the values presented[14,16].

6. RESULTS AND DISCUSSION

Mesh stiffness computed for gear pairs 2 to 7 is presented in Figs. 5(a) and 5(b). It is found from Fig. 5(a) that gear pair 3 has relatively high mesh stiffness both in the STC and DTC region. Mesh stiffness of gear pair 5 is the lowest in the double tooth contact region due to the lower coast side pressure angle and undercut on the coast side. It is observed from Figs. 5(a) and 5(b) that (i) mesh stiffness in the STC region for given coast side pressure angle is comparatively high for higher drive side pressure angle; and (ii) mesh stiffness in the STC and DTC

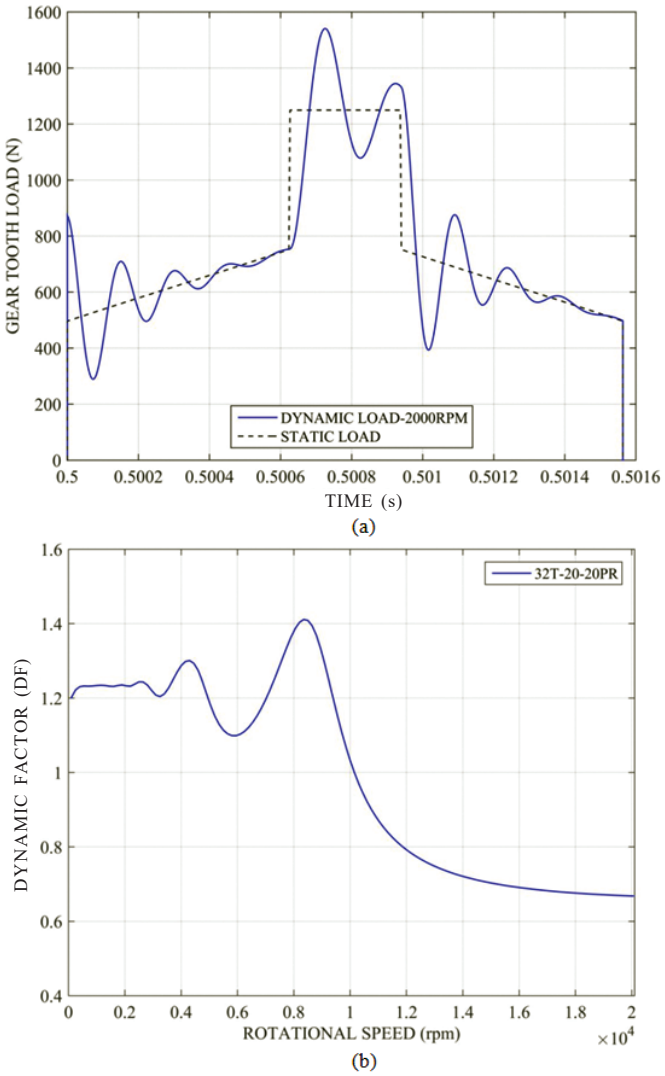

Figure 4. Static and dynamic factor of 32 teeth gear pair with parameters as per Table 1 (a) Static and dynamic tooth load at 2000 rpm (b) Change in dynamic factor with speed (mass = 1.2 kg).

zone for given drive side pressure angle is relatively low for lower coast side pressure angle.

Mesh stiffness computed under extended contact condition is presented in Figs. 6(a) and 6(b). Discontinuity seen in mesh stiffness in the extended contact zone is due to the difference in contact points during off-line and on-line of contact.

Figures 7(a) and 7(b) presents the STE under ETC condition for gear pairs 2 to 7 during the meshing cycle. It is observed from the figures that STE of symmetric gear pair 2 is the lowest and STE of asymmetric gear pair 7 is relatively high. Comparatively low mesh stiffness and high normal tooth load to transmit the same torque is the reason for relatively higher STE and reduction in single tooth contact region in gear pair 7.

Figures 8(a) and 8(b) presents the static and dynamic load acting on gear tooth pair 3 during the meshing cycle at 500 rpm and 4000 rpm respectively. Unlike non-extended tooth contact, extended tooth contact shows gradual loading and release of gear tooth load during the transition from single tooth contact to double tooth contact and vice versa.

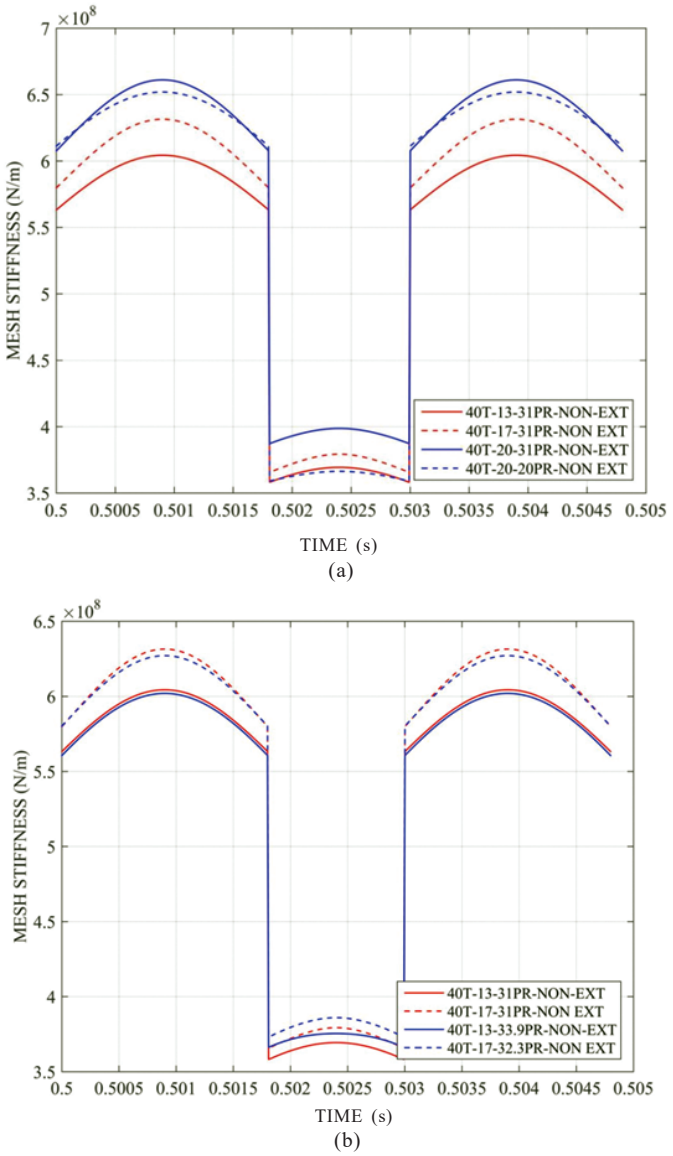

Figure 5. Mesh stiffness under non extended tooth contact computed for gear pairs 2, 3, 4, 5, 6 and 7 (a) Spur gear pairs 2, 3, 4, and 5 (b) Spur gear pairs 4, 5, 6 and 7.

Variation in dynamic factor with speed for gear tooth pair 2 and 3 presented in Fig. 9(a) shows marked difference under ETC and NETC condition till 3500 rpm. However, this difference reduces at higher speeds because the extended tooth contact region in the mesh cycle is traversed at very short time at higher speeds before the effect of ETC is felt in the system. Beyond the resonance speed, the dynamic factor drops down continually till the point of evaluation in the present study. It is demonstrated through this study that the dynamic factor of gear pair 3 is relatively lower than gear pair 2 till resonance speed. Beyond the resonance speed dynamic factor of gear pair 3 crosses over gear pair 2 and is consistently high.

Dynamic factor of gear tooth pair 2, 3, 6 and 7 is presented in Fig. 9(b). A closer study reveals the rightward shift in cross over point for gear pair 6 and 7 when compared to gear pair 3. This figure also shows that the dynamic factor of gear pair 6 and 7 is relatively lower than gear pair 2 and 3 till cross over point. Figure 9(c) shows that the difference in dynamic factor

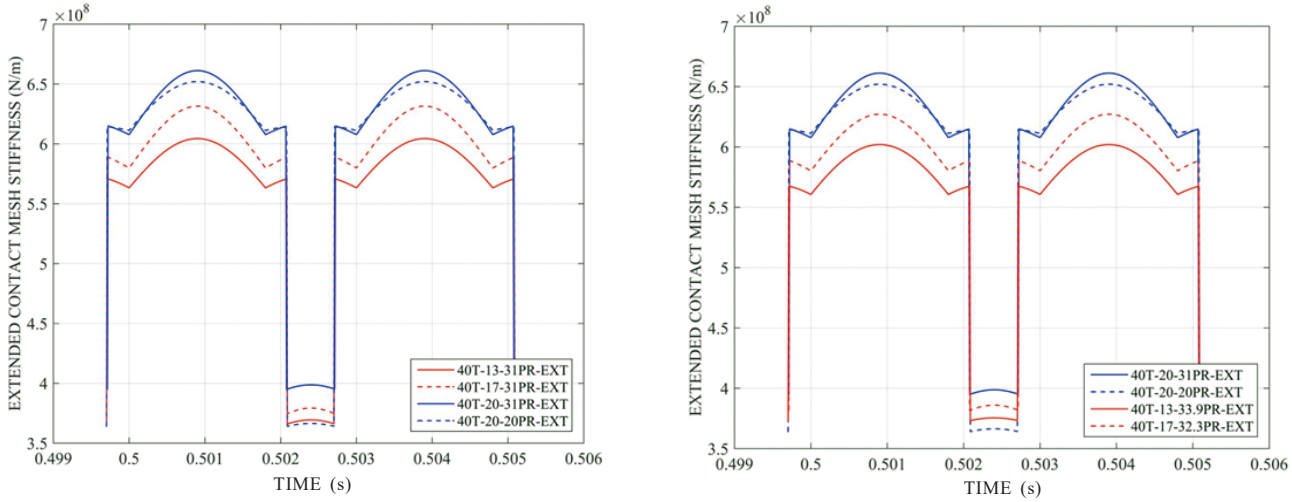

Figure 6. Mesh stiffness under extended contact computed for gear pairs 2, 3, 4, 5, 6 and 7 (a) Spur gear pairs 2,3,4 and 5 (b) Spur gear pairs 2, 3, 6 and 7.

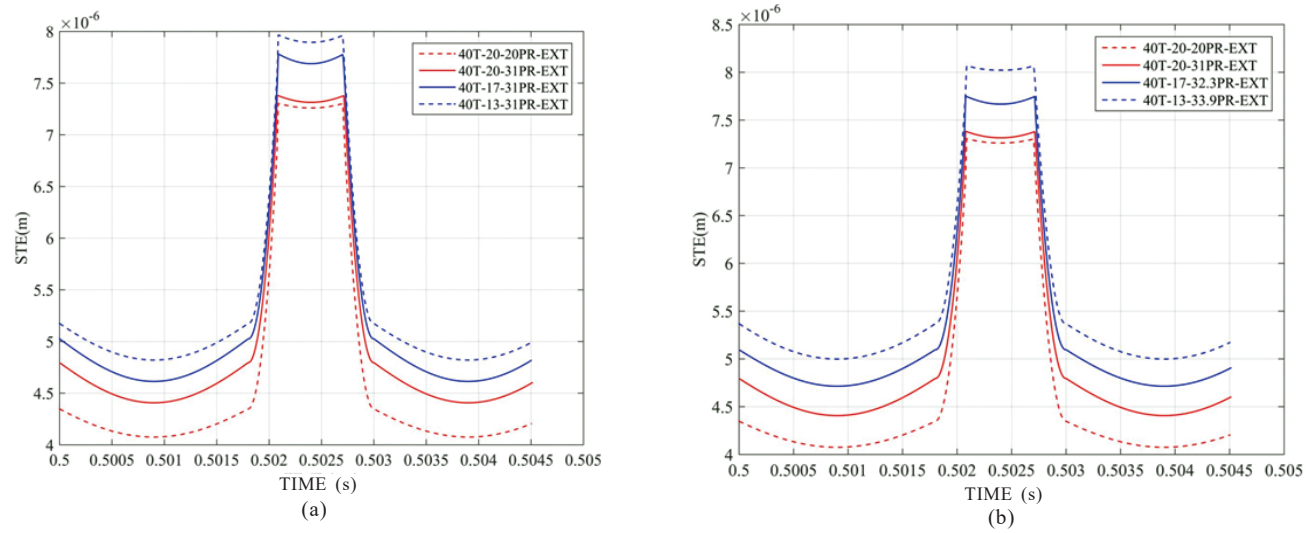

Figure 7. Static transmission error under extended tooth contact condition computed for gear pairs 2, 3, 4, 5, 6 and 7 (a) Spur gear pairs 2, 3, 4 and 5 (b) Spur gear pairs 2, 3, 6 and 7.

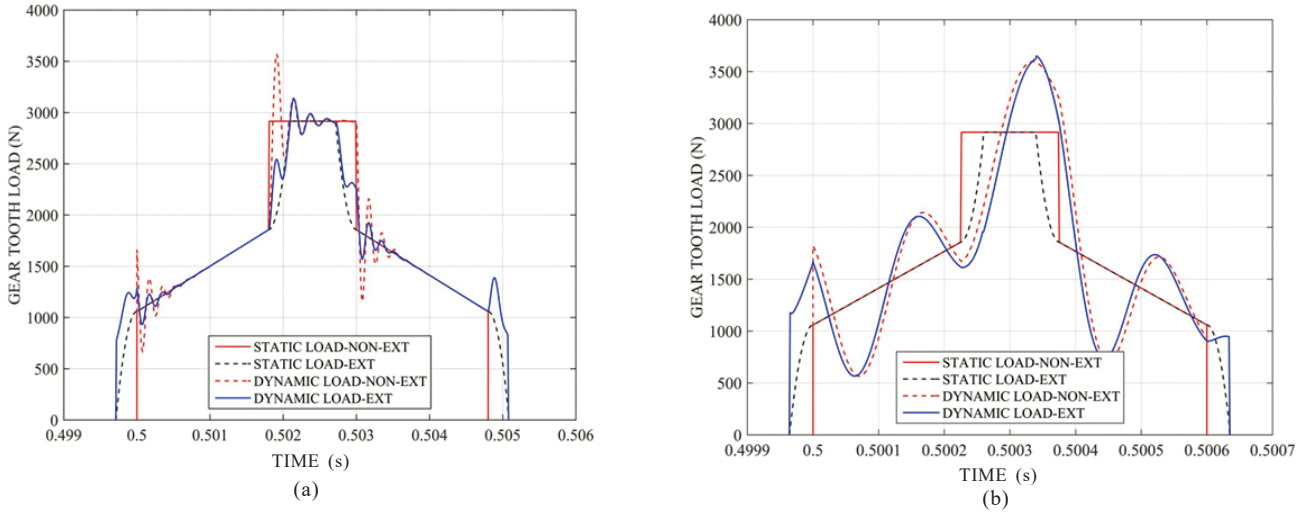

Figure 8. Static and dynamic tooth load under extended and non-extended contact condition computed for gear pair 3 (a) Static and dynamic tooth load at 500 rpm and (b) Static and dynamic tooth load at 4000 rpm.

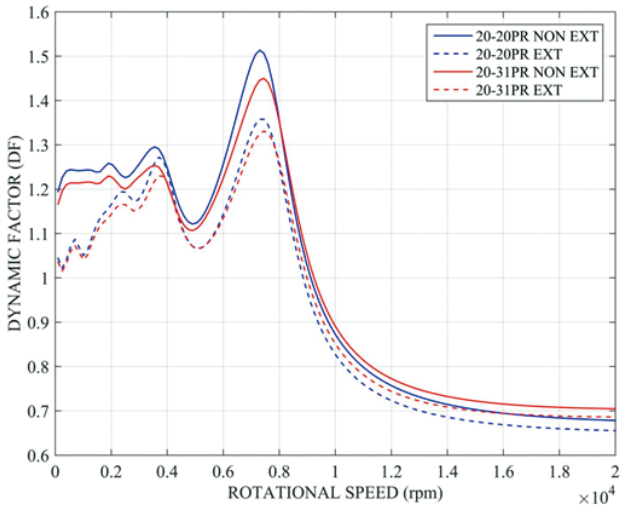

(a)

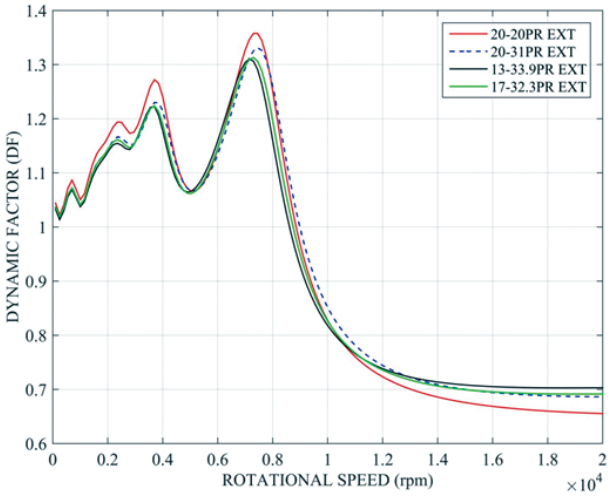

(b)

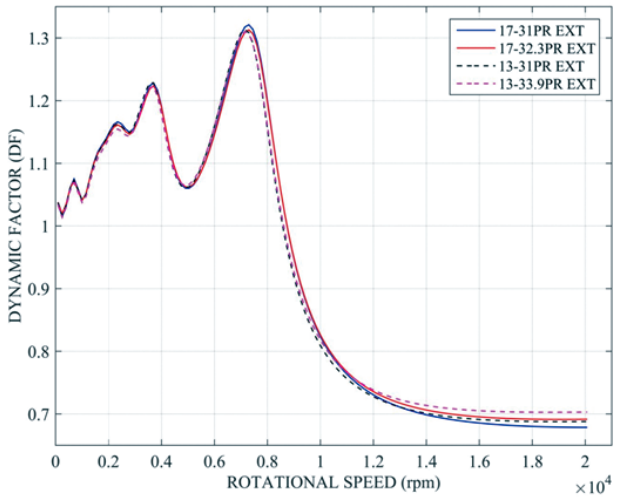

(c)

Figure 9. Variation in dynamic factor with change in speed computed for gear pairs 2, 3, 4, 5, 6 and 7 (a) Gear tooth pairs 2 and 3 under ETC and NETC condition (b) Gear tooth pairs 2, 3, 6 and 7 under ETC condition (c) Gear tooth pairs 4, 5, 6 and 7 under ETC condition.

of gear pair 4, 5, 6 and 7 across the speed range under study is relatively insignificant till cross over point.

Quasi-static motion transmission error and dynamic factor in gear pair computed analytically can be measured and validated using a four square setup consisting of test gear pair and reaction gear pair. Root strain measured using strain gauges mounted along the root radius and signals acquired using two linear accelerometers mounted tangentially and diametrically opposite on the gear blank needs to be extracted using slip rings. Signal conditioners, signal amplifiers, data acquisition board, analog to digital converter and data processing unit are some of the other instrumentation components to be used in the set up.

7. SUMMARY AND CONCLUSIONS

Primary objective of this study is to assess the influence of coast and drive side pressure angle on the dynamic behaviour of NCR, symmetric and asymmetric spur gear pair in mesh with unit gear ratio and fixed contact ratio. Conclusions based on the investigation performed on selected spur gears are summarised as follows:

i. Fixed contact ratio asymmetric gears with maximum drive side pressure angle limited by fixed top land thickness factor show increase in DTC and STC mesh stiffness with increase in coast side pressure angle. Difference in mesh stiffness at the transition from DTC to STC is minimal for the gear pair having relatively low coast side pressure angle. For fixed value of coast side pressure angle, mesh stiffness in the STC zone increases with increase in drive side pressure angle. For fixed drive side pressure angle, DTC and STC mesh stiffness increases with increase in coast side pressure.

ii. Static transmission error of NCR symmetric spur gears is relatively low in comparison with the corresponding values of asymmetric spur gears of same contact ratio.

iii. Dynamic factor of NCR asymmetric gears with maximum drive side pressure angle can be reduced by reducing the coast side pressure angle. Dynamic factor of asymmetric spur gears computed under NETC and ETC condition is relatively lower than the corresponding symmetric gear with same contact ratio till resonance speed. Beyond the resonance speed the dynamic factor of asymmetric gear crosses over and remains consistently above symmetric gear. It is found from this study that cross over point can be shifted further to higher speed by reducing the coast side pressure angle.

Findings of the present work can be used as a guideline to select the coast and drive side pressure angle of NCR asymmetric spur gears to maintain relatively low static transmission error and dynamic factor.

REFERENCES

1. Alexander L. Kapelevich &Roderick E. Kleiss, Direct gear design for spur and helical involute gears, Gear Technology, September/October 2002. https://www.geartechnology.com/issues/0902x/kapelevich.pdf
2. Thomas, Benny; Sankaranarayanasamy, K.; Ramachandra, S. & Kumar, S.P. Suresh. Search method applied for gear

tooth bending stress prediction in normal contact ratio asymmetric spur gears. *Proc IMechE Part C: J. Mech. Eng. Sci.*, 2018, **232**(24), 4647-4663. doi: 10.1177/0954406217753235

3. Lin, Hsiang-Hsi Edward & Huston, Ronald L. Dynamic loading on parallel shaft gears, NASA-CR-179473, July 1986, pp... https://ntrs.nasa.gov/archive/nasa/casi.ntrs.nasa.gov/19860018961.pdf. (Accessed on 10 October 2017)
4. Rincon, A. Fernandez del; Viadero, F.; Iglesias, M.; García, P.; de-Juan, A. & Sancibrian, R. A model for the study of meshing stiffness in spur gear transmissions. *Mech. Mach. Theory,* 2013, **61**, 30–58. doi:10.1016/j.mechmachtheory.2012.10.008
5. Pedersen, Niels Leergaard & Jorgensen, Martin Felix. On gear tooth stiffness evaluation. *Comput. Struct.,* 2014, **135**, 109–117. doi:10.1016/j.compstruc.2014.01.023
6. Karpat, Fatih; Dogan, Oguz; Yuce, Celalettin & Ekwaro-Osire, Stephen. A novel method for calculation gear tooth stiffness for dynamic analysis of spur gears with asymmetric teeth. *In* Proceedings of ASME, November, 2014, pp V04AT04A058, 8 pages. doi:10.1115/IMECE2014-39402
7. Karpat, Fatih; Dogan, Oguz; Yuce, Celalettin & Ekwaro-Osire, Stephen An improved numerical method for the mesh stiffness calculation of spur gears with asymmetric teeth on dynamic load analysis. *Adv. Mech. Eng.,* 2017, **9**(8), 1–12. doi:10.1177/1687814017721856
8. Tamminana, V.K.; Kahraman, A. & Vijayakar, S. A study of the relationship between the dynamic factors and dynamic transmission error of spur gear pairs. *J. Mech. Des.,* 2007, **129**(1),75-84. doi:10.1115/1.2359470
9. Vedmar, L. & Henriksson, B. A general approach for determining dynamic forces in spur gears. *J. Mech. Des.,* 1998, **120**(4), 593-598. doi:10.1115/1.2829320
10. Lin, Hsiang-His; Wang, Jifeng; Oswald, Fred B. &Coy, John J. Effect of extended tooth contact on the modeling of spur gear transmissions, NASA-TM-106174, E-7874, NAS 1.15:106174, ARL-TR-159, AIAA PAPER 93-2148. https://ntrs.nasa.gov/search.jsp?R=19930019222 (Accessed on 15 December 2017).
11. Coy, John J. & Chao, Charles Hu-Chih. A method of selecting grid size to account for Hertz deformation in Finite Element analysis of spur gears, NASA-TM-82623, September, 1981, Technical report AVRADCOM-TR-81-C-14. https://ntrs.nasa.gov/archive/nasa/casi.ntrs.nasa.gov/19810018987.pdf (Accessed on 1 November 2017).
12. Kasuba, R. & Evans, J.W. An extended model for determining dynamic loads in spur gearing. *J. Mech. Des.,* 1981, **103**, 399. doi: 10.1115/1.3254920
13. Lin, Hsiang Hsi & Liou, Chuen-Huei. A parametric study of spur gear dynamic, NASA/ CR-1998-206598, January 1998, Technical report ARL-CR-419. https://ntrs.nasa.gov/archive/nasa/casi.ntrs.nasa.gov/19980017427.pdf (Accessed on 03 January 2018).
14. Ekwaro-Osire, Stephen & Karpat, Fatih. Dynamic analysis of High-contact ratio spur gears with asymmetric teeth. *In* Proceedings of IMECE2008, 2008 ASME International Mechanical Engineering Congress and Exposition, October 31-November 6, USA, pp. 285-291. doi:10.1115/IMECE2008-67838
15. Karpat, Fatih; Ekwaro-Osire, Stephen & Karpat, Esin. A computer program for dynamic load simulation of spur gears with asymmetric and symmetric teeth. *World J. Mech.*, 2012, **2**, 239-245. doi:10.4236/wjm.2012.25029
16. Karpat, Fatih; Ekwaro-Osire, Stephen; Cavdar, Kadir & Babalik, Fatih C. Dynamic analysis of involute spur gears with asymmetric teeth. *Int. J. Mech. Sci.,* 2008, **50**, 1598–1610. doi:10.1016/j.ijmecsci.2008.10.004

ACKNOWLEDGMENT

Authors would like to thank Director, GTRE for his support and encouragement in performing this study.

CONTRIBUTORS

Mr Benny Thomas received his ME (Mechanical Engineering) from Indian Institute of Science, Bengaluru. Presently he is the Group Director for the Gearbox and Lubrication System group and Project Director for High speed Epicyclic gearbox at DRDO-Gas Turbine Research Establishment, Bengaluru.
Present work on asymmetric gears is a part of the studies made to enhance the performance and power density of gears used in aero-applications. Matlab code development and dynamic analysis has been carried out by him.

Dr K. Sankaranarayanasamy obtained his PhD from IIT Chennai. He is working as Professor at Mechanical Engineering Department, NIT Tiruchirappalli. His area of research includes Micro and Nano Fabrication, Composite Materials and MEMS.
Initial development of Matlab code for generation of the asymmetric gears was carried out under his supervision.

Dr S. Ramachandra holds ME (Mechanical Engineering) from Indian Institute of Science and PhD in the field of Impact Mechanics. He has experience in the field of Structural analysis and testing of aero engine components. Currently he is the Technical Director for System Engineering at DRDO-Gas Turbine Research Establishment, Bengaluru.
His contribution to the present work was to provide guidance in evolving the methodology for dynamic analysis of gear tooth.

Mr Suresh Kumar S.P. received his BSc (Mechanical Engineering) from Kerala University and has experience in high speed gearbox design and development. Currently he is the Associate Director for the Mechanical Systems and Analysis at DRDO-Gas Turbine Research Establishment, Bengaluru.
His contribution to the present work was to provide overall guidance in the initial stage of code development.